

Semantics-aware Adaptive Knowledge Distillation for Sensor-to-Vision Action Recognition

Yang Liu, Guanbin Li, *Member, IEEE*, Liang Lin, *Senior Member, IEEE*

Abstract—Existing vision-based action recognition is susceptible to occlusion and appearance variations, while wearable sensors can alleviate these challenges by capturing human motion with one-dimensional time-series signals (e.g. acceleration, gyroscope and orientation). For the same action, the knowledge learned from vision sensors (videos or images) and wearable sensors, may be related and complementary. However, there exists significantly large modality difference between action data captured by wearable-sensor and vision-sensor in data dimension, data distribution and inherent information content. In this paper, we propose a novel framework, named Semantics-aware Adaptive Knowledge Distillation Networks (SAKDN), to enhance action recognition in vision-sensor modality (videos) by adaptively transferring and distilling the knowledge from multiple wearable sensors. The SAKDN uses multiple wearable-sensors as teacher modalities and uses RGB videos as student modality. Specifically, we transform one-dimensional time-series signals of wearable sensors to two-dimensional images by designing a gramian angular field based virtual image generation model. Then, we build a novel Similarity-Preserving Adaptive Multi-modal Fusion Module (SPAMFM) to adaptively fuse intermediate representation knowledge from different teacher networks. To fully exploit and transfer the knowledge of multiple well-trained teacher networks to the student network, we propose a novel Graph-guided Semantically Discriminative Mapping (GSDM) loss, which utilizes graph-guided ablation analysis to produce a good visual explanation highlighting the important regions across modalities and concurrently preserving the interrelations of original data. Experimental results on Berkeley-MHAD, UTD-MHAD and MMAct datasets well demonstrate the effectiveness of our proposed SAKDN for adaptive knowledge transfer from wearable-sensors modalities to vision-sensors modalities.

Index Terms—Action recognition, wearable sensor, knowledge distillation, transfer learning.

I. INTRODUCTION

HUMAN action recognition has attracted increasing attention due to its wide applications such as health-care services, smart homes, intelligent surveillance and human-machine interaction, etc. With the development of deep learning, vision-sensors (images, videos) based methods dominate the community of action recognition and a large amount of effective models have been proposed and applied to real-world scenarios [1]–[3]. However, the performance of vision-based methods are easily affected by camera position, camera view-point, background clutter, occlusion and appearance variation

This work is supported in part by the China Postdoctoral Science Foundation funded project under Grant 2020M672966, and in part by the Fundamental Research Funds for the Central Universities under Grant 20lgy131. (Corresponding author: Liang Lin.)

Yang Liu, Guanbin Li and Liang Lin are with the School of Data and Computer Science, Sun Yat-Sen University, Guangzhou 510006, China. (e-mail: liuy856@mail.sysu.edu.cn, liguanbin@mail.sysu.edu.cn, linliang@ieee.org).

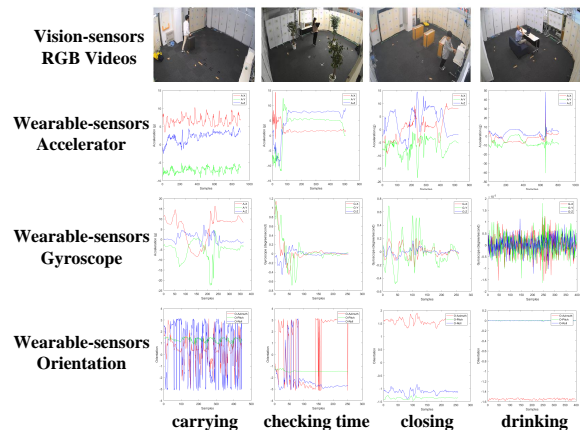


Fig. 1: Comparison of vision and wearable sensor action data.

[4]. Furthermore, vision-based methods usually require expensive hardware resources to run computationally complex computer vision algorithms [5]. In some privacy-sensitive area such as bank and government, the difficulty of acquiring images and videos make this method infeasible. However, these limitations can be addressed by low-cost and computationally efficient wearable-sensors. The wearable-sensors equipped by smartwatches or smartphones capture human actions by three-axis time-series acceleration, gyroscope and orientation signals, which are suitable for privacy protecting and robust to variance of illumination and camera view-points [4]. With the popularity and increasing demand of intelligent cities and smart health-care, human action recognition based on wearable-sensors has become a key research area in human activity understanding. Although some wearable-sensors based action recognition methods [6]–[9] have been proposed and achieved promising results, most of them just consider time-series data of wearable-sensors without considering the complementary relationship and domain divergence between vision-sensor and wearable-sensor action data. Therefore, it is considerable to leverage the knowledge from both vision-sensor and wearable-sensor modalities to improve performance of action recognition in multi-modal manner.

However, there exists significantly large modality difference between vision-sensor and wearable-sensor action data, which can be observed from Fig. 1. Obviously, the vision-sensor action data are two-dimensional images or three-dimensional videos which contains abundant color or texture information. In contrast, wearable-sensor action data are one-dimensional time-series signals without containing color and texture information. Specially, traditional action recognition methods are

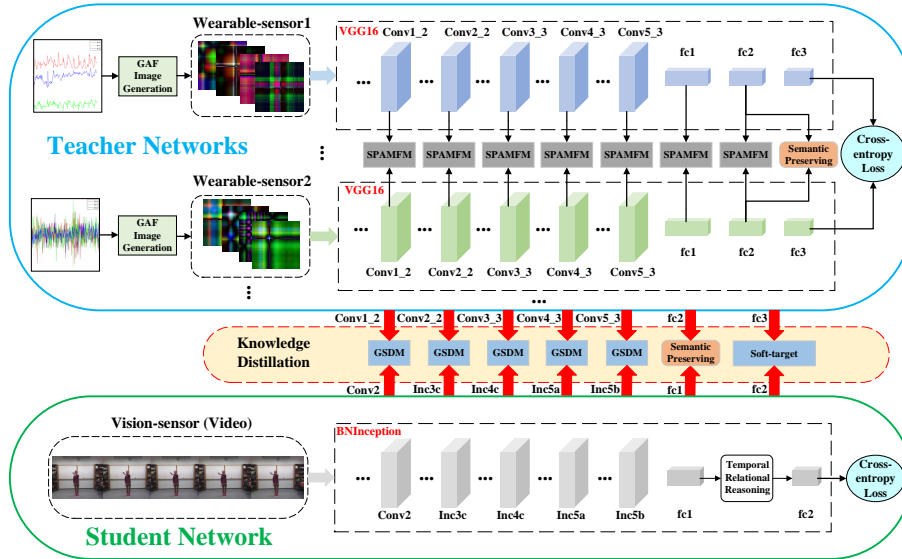


Fig. 2: Framework of our proposed method SAKDN. The Gramian Angular Field (GAF) based virtual image generation model encodes one-dimensional time-series signals of wearable-sensor into two-dimensional image representation. Similarity-Preserving Adaptive Multi-modal Fusion Module (SPAMFM) fuses intermediate representation knowledge from different teacher networks adaptively. Graph-guided Semantically Discriminative Mapping (GSDM) loss utilizes graph-guided ablation analysis to transfer the interpretable knowledge of multiple well-trained teacher networks to the student network.

usually in unimodal manner (either in vision-sensor modality or wearable-sensor modality), which is infeasible in real-world scenarios because the dynamic environment makes the model hard to adapt to the modality difference. Previous works [10]–[13] have verified the existence of complementary information between action data of vision-sensor and wearable-sensor. For instance, vision-based sensors could provide global motion features while wearable-sensors give 3D information about local body movement. Hence, by utilizing the complementary information from these two modalities, the generalization ability and the performance of action recognition can be improved. However, due to the huge modality gap between vision-sensor and wearable-sensor action data, the following three key challenges should be addressed: 1) there are multiple modalities of wearable-sensor action data, the data of each modality is one-dimensional time-series signal without containing local temporal relationship, color and texture information. This makes existing models difficult to interpret and fuse the content of multi-modal wearable-sensor action data. Therefore, specific and effective multi-modal representation learning method is needed to increase the representative power of wearable-sensor data and concurrently fuse different kinds of wearable-sensors data effectively. 2) the knowledge between wearable-sensor and vision-sensor action data is complementary. This motivates the designing of specific adaptive feature fusion method. 3) there exists large modality difference between wearable-sensor and vision-sensor action data in data dimension, data distribution and inherent information content, which highlights the importance of specific knowledge transfer method.

Based on these observations, in this paper, we focus on enhancing action recognition performance in vision-sensor modality (videos) by adaptively transferring the knowledge from multiple wearable-sensor modalities, meanwhile solving

the aforementioned challenges. In general, we propose an end-to-end knowledge distillation framework, named Semantics-aware Adaptive Knowledge Distillation Networks (SAKDN), which adaptively distill the complementary knowledge from multiple wearable-sensor modalities (teachers) to the vision-sensor modality (student), and concurrently improve the action recognition performance in vision-sensor modality (videos). An overview of the SAKDN is presented in Fig. 2. In SAKDN, we use multiple kinds of wearable-sensor signals as teacher modalities and RGB stream of video as single student modality. Since multi-modal action data share the same semantic content, we use semantics-aware knowledge of action class names to guide the multi-modal feature fusion, knowledge distillation and representation learning for SAKDN.

More specifically, the SAKDN consists of multiple teacher networks and a single student network. The acceleration, gyroscope and orientation signals are used as our teacher modalities, and the RGB videos is used as our student modality. To make the one-dimensional action data of wearable-sensor preserve local temporal relationship and facilitate its visual recognition, we build a Gramian Angular Field (GAF) [14] based virtual image generation model (as shown in Fig. 3) which transforms the one-dimensional time-series signals into two-dimensional image representations and facilitate its application to existing visual models. Since there are multiple kinds of wearable-sensors modalities, we construct a Similarity-Preserving Adaptive Multi-modal Fusion Module (SPAMFM) to fully utilize the complementary information among different teacher networks. This module utilizes the intra-modality similarity, semantic embedding and multiple relational knowledge to recalibrate the channel-wise features adaptively in each teacher network, as shown in Fig. 4. To improve the performance of the student modality, we propose

Graph-guided Semantically Discriminative Mapping (GSDM) knowledge distillation loss, which transfers the graph-guided semantics-aware attention knowledge of multiple well-trained teacher networks to guide the training of the student network, as shown in Fig. 5. Extensive experiments on three benchmarks verify that our SAKDN can realize adaptive knowledge transfer from multiple wearable-sensor modalities to vision-sensors modality and achieve state-of-the-art performance.

The main contributions of this paper are as follows:

- To fully utilize the complementary knowledge from intermediate layers of multiple teacher networks, we propose a novel plug-and-play module, named Similarity-Preserving Adaptive Multi-modal Fusion Module (SPAMFM), which integrates intra-modality similarity, semantic embeddings and multiple relational knowledge to learn the global context representation and recalibrate the channel-wise features adaptively in each teacher network.
- To effectively exploit and transfer the knowledge of multiple well-trained teacher networks to the student network, we propose a novel knowledge distillation loss, named Graph-guided Semantically Discriminative Mapping (GSDM) loss, which utilizes graph-guided ablation analysis to produce a good visual explanation highlighting the important regions in the image for predicting the semantic concept, and concurrently preserving respective interrelations of data for each modality.
- One major advantage of our method is that it exploits semantic relationship to bridge the modality gap between wearable-sensors and vision-sensors, and utilize this constraint to guide the multi-modal feature fusion, knowledge transfer and representation learning. The SAKDN focuses on the sensor-to-vision heterogenous action recognition problem and integrates SPAMFM, GSDM into a unified end-to-end adaptive knowledge distillation framework. Extensive experiments on three benchmark datasets validate the effectiveness of SAKDN.

This paper is organized as follows: Section II briefly reviews the related works. Section III introduces the proposed SAKDN. Experimental results and related discussions are presented in Section IV. Finally, Section V concludes the paper.

II. RELATED WORK

A. Uni-modal Action Recognition

Action Recognition is a very active research field and has received great attention in recent years [15] and plenty of methods have been proposed. To be noticed, most of them are based on vision-sensors modality such as RGB, depth, skeleton, infrared images or videos, etc. Some representative RGB based works include IDT [16], 3D CNN [17], two-stream CNNs [18], C3D [19], TSN [20], TRN [2], TSM [21], etc. In addition, other modalities (depth [22], [23], skeleton [24], [25], infrared [26]) based methods also receive increasing attention. Though these vision-sensors based methods have achieved promising results, their performance is easily affected by camera viewpoints, background clutter, occlusion

and illumination change. In some privacy-sensitive area such as bank and government, the difficulty of acquiring images and videos make this method infeasible. Furthermore, vision-based methods usually require expensive hardware resources to run deep learning models with high computational demands.

With the popularity of the wearable devices such as smartwatches and smartphones, human action recognition based on wearable-sensors has become a key research area in human activity understanding [8], [27]. Although aforementioned visions-sensors based methods have achieved good results, they cannot be directly applied to wearable-sensors based problems due to the existence of huge modality divergence. Since wearable-sensors action data is suitable for privacy protecting and robust to variance of illumination and camera view-points, some specific works have been proposed recently. Jiang et al. [6] assembled signal sequences of accelerators and gyroscopes into an activity image to learn optimal representations automatically. Wannenburg et al. [7] utilized ten different classifier algorithms to classify the human actions using the accelerator signals captured by smartphones. Setiawan [28] used gramian angular field to transform one-dimensional wearable-sensor signals to two-dimensional images. Wang et al. [9] proposed an attention-based CNN framework to address weakly-supervised sensors-based action recognition problem. Different from vision-sensor based methods, most of these wearable-sensor based action recognition methods are based on raw sensor time-series signals, which lacks color and texture information and could not preserve the local temporal relationship. In addition, these methods use simple feature fusion methods to fuse the knowledge from different sensor modalities without considering intra-modality similarity, semantic embeddings and multiple relational knowledge.

To increase the representative ability of wearable-sensors action features, we construct a Gramian Angular Field (GAF) based virtual image generation model, which transforms the one-dimensional time-series signals of wearable-sensors into two-dimensional image representations. To fully utilize the complementary knowledge from multiple wearable-sensors, we propose a Similarity-Preserving Adaptive Multi-modal Fusion Module (SPAMFM), which integrates intra-modality similarity, semantic embeddings and multiple relational knowledge to learn the global context representation and recalibrate the channel-wise features adaptively.

B. Multi-modal Action Recognition

Action recognition has been developed for a long period, but action recognition on multiple modalities is a relatively new topic. With the development of deep learning methods and various hardware such as cameras and wearable devices, there are some typical methods of dealing with multi-modal action recognition problems in recent years. These methods can be roughly categorized into three types: 1) cross-view action recognition, typical works [29], [30] used transfer learning methods to reduce the domain gap of action data from different camera views; 2) cross-spectral action recognition, typical works [31], [32] addressed the visible-to-infrared action recognition problems using domain adaptation methods; 3) cross-media action recognition, typical works [33], [34] designed

specific multi-modal feature learning frameworks to address the image-to-video action recognition problems.

Different from above-mentioned cross-domain action recognition problems, the multi-modal action recognition based on wearable-sensors and vision-sensors (sensor-to-vision) is essentially a heterogenous knowledge transfer problem because there exists large modality difference between wearable-sensors and vision-sensors in data dimension, data distribution and inherent information content, which is shown in Fig. 1. And related research about sensor-to-vision action recognition is limited. Chen et al. [35] proposed a feature fusion framework to combine signals from depth camera and inertial body sensor. Kong et al. [4] built a multi-modality distillation model with attention mechanism to realize adaptive knowledge transfer from sensor modalities to vision modalities. Hamid et al. [36] proposed a multi-modal transfer module to fuse knowledge from different unimodal CNNs and tested this module for three different multi-modal fusion tasks: gesture recognition, audio-visual speech enhancement and action recognition. However, most of these methods only use raw one-dimensional time-series sensor signals to recognize actions. Since time-series data lacks local temporal relationship, color and texture information, it may affect the representative ability of wearable-sensor signals and make existing pre-trained deep learning models (e.g. LeNet, AlexNet, VGGNet, ResNet, etc.) hard to adapt. Furthermore, the semantic relationship between wearable-sensors and vision-sensors action data is ignored in previous works, which can guide the knowledge transfer.

In this paper, we use the semantics-aware information to guide the multi-modal feature fusion, knowledge distillation and representation learning of our SAKDN. Although method [36] built a squeeze and excitation based multi-modal feature fusion module which only used the simple concatenation of features from different modalities to learn the global context embedding without considering more diverse relation functions and the intra-modality similarity relationship. Differently, we propose a novel plug-and-play module, named Similarity-Preserving Adaptive Multi-modal Fusion Module (SPAMFM), which seamlessly integrates intra-modality similarity, semantic emdeddings and multiple relational knowledge to learn the global context representation and recalibrate the channel-wise features adaptively in each network.

C. Knowledge Distillation

Knowledge distillation is a general technique for supervising the training of student networks by capturing and transferring useful knowledge from well-trained teacher networks. Hinton et al. [37] used softened labels of the teacher with a temperature to transfer knowledge to a small student network. Attention transfer [38] designed a knowledge distillation loss based on summed p -norm of convolutional feature activations along channel dimension. Park et al. [39] proposed distance-wise and angle-wise distillation losses to realize relational knowledge transfer. Tung et al. [40] construct a knowledge distillation loss with the constraint that input pairs which produce similar (dissimilar) activations in the teacher network should produce similar (dissimilar) activations in the student

network. Hoffman et al. [41] built a modality hallucination architecture for training an RGB object detection model using depth as side information. Garcia et al. [42] proposed a generalized distillation framework considering the case of learning representations from depth and RGB videos, while relying on RGB data only at test time. Crasto et al. [43] introduced a feature-based loss compared to the Flow stream, a linear combination of the feature-based loss and the standard cross-entropy loss, to mimic the motion stream, and as a result avoids flow computation at test time. Different from existing knowledge distillation methods that focus on modality transfer task across vision-sensor based modalities, we move a further step towards knowledge transfer from wearable-sensor based modalities to vision-sensors based modalities. In this paper, we construct a novel knowledge distillation loss, named Graph-guided Semantically Discriminative Mapping (GSDM) loss, which utilizes graph-guided ablation analysis to produce a good visual explanations highlighting the important regions for predicting the semantic concept and preserving the intrinsic structures concurrently. Since semantic relationship between wearable-sensors and vision-sensors is similar, we transfer the semantics-aware attention knowledge of multiple well-trained teacher networks to guide the training of the student network.

III. SEMANTICS-AWARE ADAPTIVE KNOWLEDGE DISTILLATION NETWORKS

A. Framework Overview

The framework of the SAKDN is shown in Fig. 2, which is an end-to-end knowledge distillation framework seamlessly constituted by three parts: virtual image generation of wearable-sensors, training of multiple teacher networks, and multi-modality knowledge distillation from multiple teacher networks to the student network. We use wearable-sensors action data (acceleration, gyroscope and orientation) as teacher modalities, and RGB videos as student modality. The backbone of our teacher modality is VGGNet [44] while our student modality use TRN [2] with BN-Inception. The virtual image generation part uses Gramian Angular Field (GAF) [14], [28] to encode one-dimensional time-series signals of wearable-sensor into two-dimensional image representation while concurrently preserving the local temporal relationship information. Since there are multiple teacher modalities, we build a novel Similarity-Preserving Adaptive Multi-modal Fusion Module (SPAMFM) to fuse intermediate representation knowledge from different teacher networks adaptively. This module can be added into multiple teacher networks in plug-and-play manner, and then we use semantic preserving loss along with cross-entropy loss for the training of multiple teacher networks. The multi-modality knowledge distillation consists of two knowledge distillation loss, one is our proposed Graph-guided Semantically Discriminative Mapping (GSDM) loss which can utilizes graph-guided ablation analysis to produce a good visual explanations highlighting the important regions in the image for predicting the semantic concept and concurrently exploiting and transfer the interpretable knowledge of multiple well-trained teacher networks to the student network, the other one is the soft-target knowledge distillation

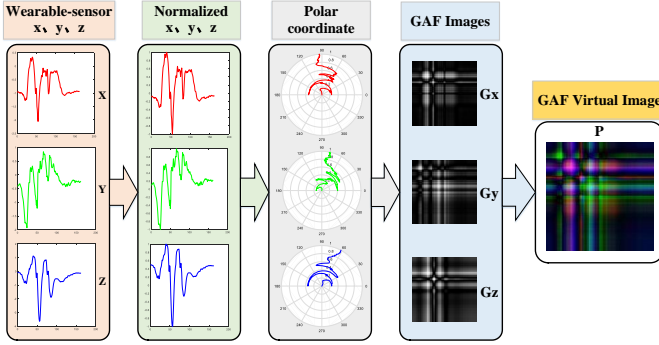


Fig. 3: Overview of Gramian Angular Field (GAF) based virtual image generation framework.

loss [37]. We train the student network using GSDM loss, soft-target loss along with semantic preserving loss and cross-entropy loss.

B. Virtual Image Generation

The Gramian Angular Field (GAF) based virtual image generation model is shown in Fig. 3. Since there are three axial time-series signals (x, y, z) of wearable-sensors action data, we denote one of the tri-axial signals as $X = \{x_1, \dots, x_n\}$. We then use min-max normalization to normalize original signal X into the interval $[-1, 1]$ and get normalized signal \tilde{X} ,

$$\tilde{X}_i = \frac{(x_i - \max(X)) + (x_i - \min(X))}{\max(X) - \min(X)} \quad (1)$$

Then, we use transformation function g to transform the normalized signal \tilde{X} to polar coordinate system, which represents cosine angle from the normalized amplitude and the radius from the time t , as represented in Eq. (2).

$$g(\tilde{x}_i, t_i) = [\theta_i, r_i] \quad \text{where} \quad \begin{cases} \theta_i = \arccos(\tilde{x}_i), \tilde{x}_i \in \tilde{X} \\ r_i = t_i \end{cases} \quad (2)$$

After encoding the normalized time-series signals into polar coordinate system, the correlation coefficient between time intervals can be easily obtained by trigonometric sum between points. Since the correlation coefficient can be calculated by the cosine of the angle between vectors [14], [28], the correlation between time i and j is calculated using $\cos(\theta_i + \theta_j)$ and the Gramian Angular Field based matrix is defined as G :

$$G = \begin{pmatrix} \cos(\theta_1 + \theta_1) & \cdots & \cos(\theta_1 + \theta_n) \\ \vdots & \ddots & \vdots \\ \cos(\theta_n + \theta_1) & \cdots & \cos(\theta_n + \theta_n) \end{pmatrix} \quad (3)$$

In this way, the GAF provides a new representation style which can preserve the local temporal relationship in the form of temporal correlation as the timestamp increases. In wearable-sensor based action recognition, the accelerator, gyroscope and orientation signals are in tri-axial style. Therefore, we assume that each axis sensor data with length n can be transformed into a single GAF matrix with the size $n \times n$. Then, the GAF matrices of tri-axial sensor data (x-, y-, and z-axis) are assembled as a three channel image representation

$P = \{G_x, G_y, G_z\}$ of size $n \times n \times 3$. And this novel image representation is named as GAF based Virtual Image (GAFVI). GAFVI of wearable-sensors will be used as the input for teacher modalities in this paper.

C. Similarity-Preserving Adaptive Multi-modal Fusion

To fully utilize the complementary knowledge from multiple teacher modalities, we will discuss our proposed Similarity-Preserving Adaptive Multi-modal Fusion Module (SPAMFM), which integrates intra-modality similarity, semantic embeddings and multiple relational knowledge to learn the global context representation and recalibrate the channel-wise features adaptively in each teacher network. The simplest case of SPAMFM for two modalities is shown in Fig. 4.

1) *Intra-modality Similarity Matrix Generation*: Assume that we have m teacher modalities and each modality has its own network $\{T_k | k = 1, \dots, m\}$. Given an input mini-batch of size b , the activation map produced by the teacher network T_k at a particular layer l is denoted as $A_{T_k}^l \in \mathbb{R}^{b \times c_k \times h_k \times w_k}$, where b is the batch size, c_k is the number of output channels for the k -th modality, and h_k, w_k are spatial dimensions. Inspired by attention-based knowledge transfer methods [38], [40] which use activation correlation to conduct knowledge transfer, we use min-batch data to calculate intra-modality similarities in particular intermediate layers for different teacher modalities. Specifically, the activation maps $A_{T_k}^l$ are first reshaped to $R_{T_k}^l \in \mathbb{R}^{b \times c_k h_k w_k}$, and then we use row-wise L2-normalized outer product of $R_{T_k}^l$ matrices to calculate intra-modality similarity-preserving matrices $G_{T_k}^l \in \mathbb{R}^{b \times b}$:

$$\tilde{R}_{T_k}^l = R_{T_k}^l \times R_{T_k}^{l\top} \quad (4)$$

$$G_{T_k}^l[i, :] = \frac{\tilde{R}_{T_k}^l[i, :]}{\left\| \tilde{R}_{T_k}^l[i, :] \right\|_2} \quad (5)$$

where $\tilde{R}_{T_k}^l$ encodes the similarity of the activations within teacher modality k of layer l in the mini-batch, $[i, :]$ denotes the i -th row in a matrix. These intra-modality similarities $G_{T_k}^l[i, :]$ can be utilized as weight matrices to guide the fusing of different relation functions in global context modeling. In this way, the calculated global context information can adaptively preserve intra-modality relationship as well as the complementary information among different teacher modalities.

2) *Global Context Modeling and Feature Recalibration*: After obtaining the intra-modality similarity matrices $\{G_{T_k}^l | k = 1, \dots, m\}$, we build a global context modeling module to receive features from particular layers (conv or fc) of different teacher networks and learns a similarity-preserved global context embedding, then we use this embedding to recalibrate the input features from different modalities. To fix notation, we let $A_k^l \in \mathbb{R}^{b \times c_k \times h_k \times w_k}$ denotes the feature maps of a batch at a given layer l of modality k . We first use global average pooling (GAP) to generate squeezed feature vectors $S_k^l \in \mathbb{R}^{b \times c_k}$ for different modalities. Formally, a statistic S_k^l is

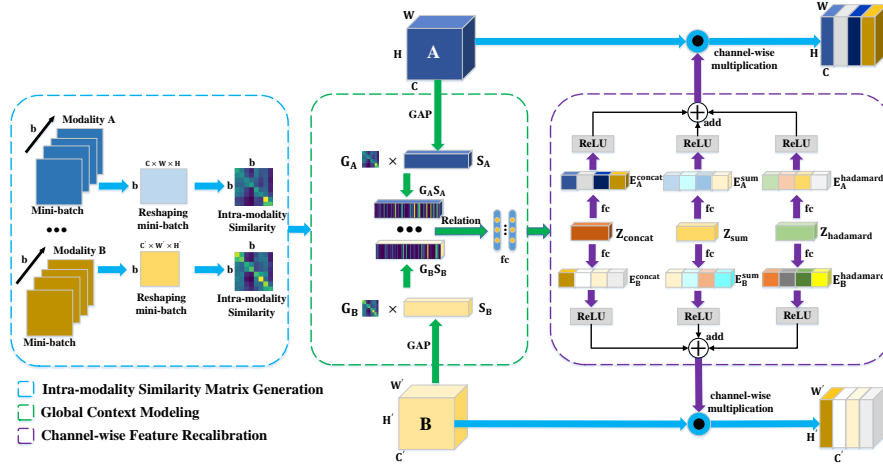


Fig. 4: Architecture of SPAMFM for two modalities. A and B denote the features at a given layer of two CNNs.

generated by shrinking A_k^l through spatial dimensions $h_k \times w_k$, where the c -th element of S_k^l is calculated by:

$$S_k^l(b, c) = \frac{1}{h_k \times w_k} \sum_{i=1}^{h_k} \sum_{j=1}^{w_k} A_k^l(b, c, i, j) \quad (6)$$

In order to make the global context preserve intra-modality relationship as well as the complementary information among different teacher modalities, we use the product of intra-modality similarity matrix $G_{T_k}^l$ and squeezed feature vector S_k^l for each teacher modality to learn joint representation. To aggregate their complementary heterogenous information from different aspects, we use three different relation functions: concatenation, summation and hadamard product, which have been validated their effectiveness in [45]. Thus, we can get three forms of joint representations through three independent fully-connected layers with three kinds of relation functions:

$$Z_{con}^l = W_{con1}^l [G_{T_1}^l S_1^l, \dots, G_{T_m}^l S_m^l] + b_{con1}^l \quad (7)$$

$$Z_{sum}^l = W_{sum1}^l \left(\sum_{k=1}^m G_{T_k}^l S_k^l \right) + b_{sum1}^l \quad (8)$$

$$Z_{had}^l = W_{had1}^l \prod_{k=1}^m G_{T_k}^l S_k^l + b_{had1}^l \quad (9)$$

where $[\cdot, \cdot]$ denotes the concatenation operation, $\prod_{k=1}^m$ denotes hadamard product from modality 1 to modality m , $Z_{con}^l \in \mathbb{R}^{c_{con}}$, $Z_{sum}^l \in \mathbb{R}^{c_{sum}}$ and $Z_{had}^l \in \mathbb{R}^{c_{had}}$ denote joint representations of l -th layer for concatenation, summation and hadamard product relation functions, respectively. Here, $W_{con1}^l \in \mathbb{R}^{c_{con} \times \sum_{k=1}^m c_k}$, $W_{sum1}^l \in \mathbb{R}^{c_{sum} \times c_k}$, $W_{had1}^l \in \mathbb{R}^{c_{had} \times c_k}$ are weights, $b_{con1}^l \in \mathbb{R}^{c_{con}}$, $b_{sum1}^l \in \mathbb{R}^{c_{sum}}$ and $b_{had1}^l \in \mathbb{R}^{c_{had}}$ are the biases of the fully-connected layers. We choose $c_{con} = \frac{\sum_{k=1}^m c_k}{2m}$, $c_{sum} = c_k$ and $c_{had} = c_k$ according to [46] to restrict the model capacity and increase its generalization ability.

To make use of the global context information aggregated in the above three joint representations Z_{con}^l , Z_{sum}^l and Z_{had}^l , we

predict excitation signals for them through three independent fully-connected layers:

$$E_{con}^l = W_{con2}^l Z_{con}^l + b_{con2}^l \quad (10)$$

$$E_{sum}^l = W_{sum2}^l Z_{sum}^l + b_{sum2}^l \quad (11)$$

$$E_{had}^l = W_{had2}^l Z_{had}^l + b_{had2}^l \quad (12)$$

where $W_{con2}^l \in \mathbb{R}^{c_k \times c_{con}}$, $W_{sum2}^l \in \mathbb{R}^{c_k \times c_{sum}}$, $W_{had2}^l \in \mathbb{R}^{c_k \times c_{had}}$ are weights, $b_{con2}^l \in \mathbb{R}^{c_k}$, $b_{sum2}^l \in \mathbb{R}^{c_k}$ and $b_{had2}^l \in \mathbb{R}^{c_k}$ are the biases of the fully connected layers.

After obtaining these three excitation signals $E_{con}^l \in \mathbb{R}^{c_k}$, $E_{sum}^l \in \mathbb{R}^{c_k}$ and $E_{had}^l \in \mathbb{R}^{c_k}$, we use them to recalibrate the input feature A_k^l from each modality k adaptively by a simple gating mechanism,

$$\tilde{A}_k^l = (\delta(E_{con}^l) + \delta(E_{sum}^l) + \delta(E_{had}^l)) \odot A_k^l \quad (13)$$

where \odot is channel-wise product operation for each element in the channel dimension, and $\delta(\cdot)$ is the ReLU function. With SPAMFM, we can realize adaptive multi-modal feature fusion and inter-modality feature recalibration, which allows the features of one modality to recalibrate the features of another modality while concurrently preserving the intra-modality similarities as well as the complementary information among different teacher modalities.

D. Graph-guided Semantically Discriminative Mapping

To mitigate the modality divergence between teacher and student modalities, we propose a novel semantics-aware knowledge distillation loss, named Graph-guided Semantically Discriminative Mapping (GSDM), which works at convolutional layers and transfers the semantics-aware attention knowledge of multiple well-trained teacher networks to guide the training of student network. This loss utilizes graph-guided ablation analysis to produce a good visual explanations for both teacher and student modalities highlighting the important regions for predicting the semantic concept, and concurrently preserving respective interrelations of data for each modality. Since previous works [47]–[49] have validated that the ablation of some units of a network can be an indicator

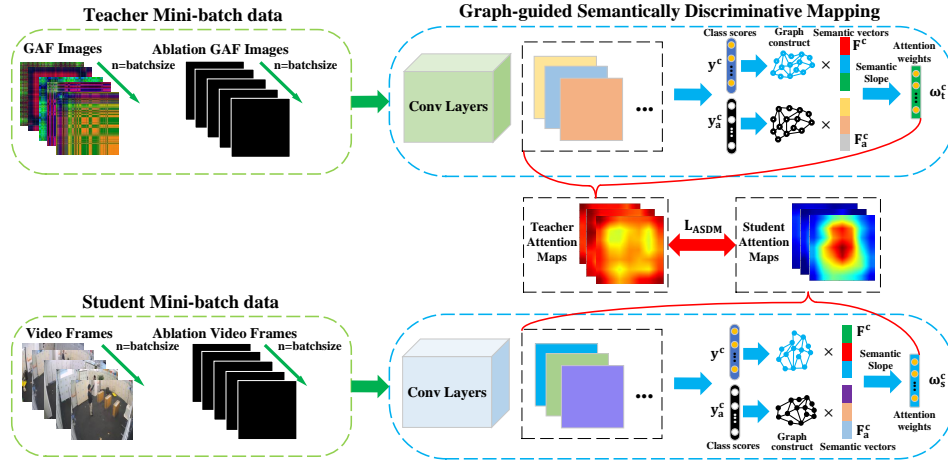


Fig. 5: Overview of Graph-guided Semantically Discriminative Mapping (GSDM) knowledge distillation loss.

of how important a unit is for a particular class, we use ablation drop of min-batch input features to produce visual explanations based knowledge distillation loss across domains. Different from previous methods which use global average pooled gradients and class scores for visual explanation, we use semantics-guided ablation analysis to learn the visual explanations because the similar semantic relationship between wearable-sensors and vision-sensors data can be considered as good guidance for knowledge transfer while class scores is too strict for heterogenous sensor-to-vision action recognition problem. The framework of GSDM is shown in Fig. 5.

The input mini-batch data of student network contains two parts, the first part $I \in \mathbb{R}^{b \times c \times h \times w}$ contains raw input mini-batch data, the second part $I_a \in \mathbb{R}^{b \times c \times h \times w}$ contains black images which is essentially the ablation of the raw input data. And the combination of these two parts $[I; I_a] \in \mathbb{R}^{2b \times c \times h \times w}$ is used as the input. We assume that the class score y^c for class c can be considered as a non-linear function of input data. When we set all the input mini-batch data to zeros and repeat the forward pass, we get a reduced activation score y_a^c with respect to feature map A_p of p -th unit. Based on these class scores y^c and y_a^c , we use Glove [50] to calculate their corresponding semantic embeddings F^c and F_a^c :

$$F = \begin{cases} F^c = \text{Glove}(y^c) \in \mathbb{R}^{b \times 300}, & \text{when input is } I; \\ F_a^c = \text{Glove}(y_a^c) \in \mathbb{R}^{b \times 300}, & \text{when input is } I_a. \end{cases} \quad (14)$$

To extract the intrinsic structures for both original data I and ablation data I_a , we construct two graphs for them respectively, where vertexes are embedded features at the final fully connected layers and edges are the relations between features. The edge weights $W_{i,j}$ between the input data x_i and x_j are determined by the Gaussian similarity, $W_{i,j} = \exp(-\frac{\|f_i - f_j\|^2}{2})$, where f_i and f_j are embedded feature vectors of x_i and x_j . Then we apply the normalized graph Laplacians [51] on W , that is, $Q = D^{1/2}WD^{-1/2}$, where D is a diagonal matrix with its (i, i) -value to be the sum of the i -th row of W . In this way, the manifold structure in the data can be well represented in graph matrix $Q \in \mathbb{R}^{b \times b}$.

To preserve the intrinsic structures of original modalities when conduct knowledge distillation, we first multiply the

semantic embeddings with the graph matrix, which has been validated its effectiveness in [52]. Then, we define a graph-guided slope metric $\omega_{p,l}^c \in \mathbb{R}^{b \times 300}$ to measure the changing rate of the transformed semantic embeddings for the p -th unit of layer l and class c .

$$\omega_{p,l}^c = \frac{QF^c - Q_a F_a^c}{QF^c} \quad (15)$$

where $Q \in \mathbb{R}^{b \times b}$ and $Q_a \in \mathbb{R}^{b \times b}$ are the normalized graph similarity matrices for original data and ablation data, respectively. In this way, the intrinsic of data can be preserved and concurrently the importance value can be represented by the fraction of drop in semantic embeddings of class c when the input features are removed. Then the graph-guided semantically discriminative map M_l^c for the l -th layer of class c can be obtained as weighted linear combination of activation maps $A_{p,l}$ and corresponding weights $\omega_{p,l}^c$,

$$M_{p,l}^c = \text{ReLU} \left(\sum_p \omega_{p,l}^c A_{p,l} \right) \quad (16)$$

The dimensionality of the weight $\omega_{p,l}^c$ is adaptively adjusted to the dimensionality of different feature maps in the same way as the Grad-CAM [53]. The GSDM of specific layers for teacher and student networks are generated following Eq. (16). After obtaining the GSDM, the GSDM based knowledge distillation loss can be constructed. Assume that we have m teacher modalities and one student modality, we use mean squared error (MSE) loss between the normalized GSDM of teachers and student to transfer knowledge:

$$L_{\text{GSDM}} = \frac{\sum_{k=1}^m \sum_{l_T \in \mathcal{L}_{\text{distill}}^T, l_S \in \mathcal{L}_{\text{distill}}^S} \left\| \frac{M_{l_T}^{T_k}}{\|M_{l_T}^{T_k}\|_2} - \frac{M_{l_S}^S}{\|M_{l_S}^S\|_2} \right\|_2^2}{m \times N \mathcal{L}_{\text{distill}}^T} \quad (17)$$

where $M_{l_T}^{T_k}$ denotes the GSDM for teacher network T_k of the l -th layer, $M_{l_S}^S$ is the GSDM for student network of the l -th layer, $\mathcal{L}_{\text{distill}}^T$ represents the group containing the choosing layers of teacher networks for knowledge distillation, $\mathcal{L}_{\text{distill}}^S$ is the group containing the choosing layers of student network,

and $\|\cdot\|_2$ denotes the L2 norm. $N^{\mathcal{L}_{distill}^T}$ is the number of choosing layers in group $\mathcal{L}_{distill}^T$.

E. Semantics-aware Adaptive Knowledge Distillation

Based on Virtual Image Generation model, Similarity-Preserving Adaptive Multi-modal Fusion Module (SPAMFM) and Graph-guided Semantically Discriminative Mapping (GSDM) knowledge distillation loss, we seamlessly integrates them into a unified end-to-end adaptive knowledge distillation framework, named, Semantics-aware Adaptive Knowledge Distillation Network (SAKDN), to address the sensor-to-vision heterogenous action recognition problem, as shown in Fig. 2. In SAKDN, we use multiple wearable-sensors as teacher modalities and use vision-sensor as student modality. For teacher networks, the input is GAF images of wearable-sensors. And the input of student network is RGB videos.

1) *Training of teacher networks:* Assume that we have m wearable-sensors modalities, we build m teacher networks using VGG16 [44] as the backbone. As shown in Fig. 2, given GAF images for each modality, we simultaneously feed them into their respective networks for model training. The SPAMFM are added into selected layers of VGG16 among teacher networks, which is shown as follows:

$$\mathcal{L}_{SPAMFM} = \{\text{conv}_1^2, \text{conv}_2^2, \text{conv}_3^3, \text{conv}_4^3, \text{conv}_5^3, \text{fc1}, \text{fc2}\} \quad (18)$$

In addition to the SPAMFM, we design a semantic preserving loss at fc2 layer among different teacher networks to make sure the fc2 layer contain semantic knowledge as well as the intra-modality relationship and the complementary information from different teacher modalities. The semantic preserving loss L_{SP}^T is defined as the MSE loss between the raw features of the fc2 layer and their corresponding semantic representations of action class names,

$$L_{SP}^T = \frac{1}{m} \sum_{k=1}^m \|H_k^T - F_k\|_2^2 \quad (19)$$

where H_k^T is the raw feature of the fc2 layer for teacher network k , F_k is the corresponding semantic representation.

All the teacher networks are trained simultaneously using L_{SP}^T along with the summation of cross-entropy loss for all teacher networks L_{CS}^T . The total loss L_T for all teacher networks is organized as:

$$L_T = L_{CS}^T + L_{SP}^T = \frac{1}{m} \sum_{k=1}^m \text{CE}(Y_k^T, Z_k^T) + \frac{1}{m} \sum_{k=1}^m \|H_k^T - F_k\|_2^2 \quad (20)$$

where CE is the cross entropy, Y_k and Z_k denote the predicted labels and class probability for teacher network k , respectively.

2) *Training of student network:* Our student network is a TRN [2] with BN-Inception using only RGB videos as input. During the training of student network, the parameters of teacher networks are fixed, as shown in Fig. 2. In order to reduce the computational cost during the training phase, we only perform distillation on some representative features. Thus, the GSDM are added into selected convolutional layers

between BN-Inception and VGG16 networks for all teacher-student pairs, which are shown as follows:

$$\mathcal{L}_{distill}^T = \{\text{conv}_1^2, \text{conv}_2^2, \text{conv}_3^3, \text{conv}_4^3, \text{conv}_5^3\} \quad (21)$$

$$\mathcal{L}_{distill}^S = \{\text{conv2}, \text{Inc3c}, \text{Inc4c}, \text{Inc5a}, \text{Inc5b}\} \quad (22)$$

where conv_i^j represents the j -th convolutional activation map of convolution group i , Inc represents the inception layer.

In addition to the GSDM distillation loss L_{GSDM} in Eq. (17), we build a complementary knowledge distillation loss at the last fully-connected layers between teacher and student networks.

$$L_{ST} = \frac{1}{m} \sum_{k=1}^m \text{KL}\left(\frac{P_k^T}{T}, \frac{P_k^S}{T}\right) \quad (23)$$

where $\text{KL}(\cdot, \cdot)$ is the Kullback-Leibler divergence, P_k^T is the class probability prediction of teacher network k , P_k^S is the class probability prediction of the student network, T denotes the temperature controlling the distribution of the probability. We set $T = 4$ in this paper suggested by [37].

To make the semantic knowledge between teacher and student networks similar, we use semantic preserving loss between fc1 layer of the student network and fc2 layer of teacher networks, which is defined as follows:

$$L_{SP}^S = \frac{1}{m} \sum_{k=1}^m \|H^S - H_k^T\|_2^2 \quad (24)$$

where H^S denotes the features of fc1 layer for student network, H_k^T represent the features of the fc2 layer for teacher network k . Since we use Eq. (19) to train the teacher networks, the fc2 layer of the trained teacher network already contains semantic knowledge. Therefore, we can realize semantic knowledge preserving for student network using Eq. (24).

To train the student network, we use cross entropy loss $L_{CS}^S = \text{CE}(Y^S, Z^S)$ along with two knowledge distillation loss L_{GSDM} and L_{ST} , and semantic preserving loss L_{SP}^S . The total loss L_S for student network is defined as follows:

$$L_S = L_{CS}^S + \alpha L_{ST} + \beta L_{GSDM} + \gamma L_{SP}^S \quad (25)$$

where Y^S and Z^S are predicted labels and class probability for student network, respectively. α , β and γ are the parameters controlling importance of ST, GSDM and SP loss.

IV. EXPERIMENTS

A. Experimental Setup

In this work, we conduct extensive experiments on three benchmarks for sensor-to-vision action recognition. We first introduce the three datasets and implementation details. Then, we conduct ablation studies to analyze the importance of the proposed SPAMFM, GSDM and SP. In addition, we conduct experiments with different backbone architectures and selected transfer layers to validate whether our SAKDN could generalize to different networks and choosing layers. Furthermore, we use grid-search method to conduct parameter sensitivity analysis of hyper-parameters α , β and γ in three datasets. Finally, we compare our SAKDN with existing knowledge distillation and action recognition methods.

TABLE I: Implementation details for three benchmark datasets. Batch denotes the batch size, LR is the initial learning rate, DR is the decay ratio of learning rate, DI is the decay iterations of the learning rate, Iters is the total iterations.

Dataset	Modality	Batch	LR	DR	DI	Iters
Berkeley-MHAD	Teacher	8	0.0001	0.5	50	100
	Student	8	0.001	0.1	20	30
UTD-MHAD	Teacher	16	0.0002	0.5	50	100
	Student	16	0.001	0.5	50	100
MMAct	Teacher	16	0.0001	0.5	50	70
	Student	32	0.001	0.5	30	60

1) *Berkeley-MHAD* [54]: This dataset consists of 11 action classes performed by 12 subjects with 5 repetitions for each action. There are 12 different camera views in total. The action data modalities include RGB videos, depth images, accelerators and microphones. In this paper, we use RGB videos and accelerators. There are 7,900 RGB videos and 6 different accelerator modalities. Each accelerator modality has 658 samples and the total number of accelerator samples are 3,948. In all experiments, we use the first 7 subjects for training and the last 5 subjects for testing.

2) *UTD-MHAD* [55]: It consists of 27 different actions performed by 8 subjects with 4 repetitions. This dataset has five modalities: RGB, depth, skeleton, Kinect and inertial data. The vision-sensors data are captured by Kinect camera, while wearable-sensors data are captured by inertial sensor. In this paper, we use RGB videos and two different wearable-sensors modalities (accelerator, gyroscope). Each modality has 861 samples. Since each subject performs an action for 4 times, we choose the first two samples of each action to form the training set and the remaining samples as the testing set.

3) *MMAct* [4]: MMAct is a large-scale multi-modal action dataset consist of more than 36,000 trimmed clips with seven modalities captured by 20 subjects, which include RGB videos, keypoints, acceleration, gyroscope, orientation, Wi-Fi and pressure signal. Each modality has 37 action classes. This dataset is challenge as it contains 4 camera views combining with random walk and occlusion scene. In this paper, we use RGB videos and four different wearable-sensors modalities (accelerator-phone, accelerator-watch, gyroscope and orientation). We use four different settings to evaluate this dataset: cross-subject, cross-view, cross-scene and cross-session according to the train-test split strategy in [4].

For teacher networks, we used VGGNet16 [44] as backbone. For student network, we adopt multi-scale TRN [2] with BN-Inception pretrained on ImageNet because of its balance between accuracy and efficiency. In the multi-scale TRN, we set the dropout ratio as 0.8 after the global pooling layer to reduce the effect of over-fitting, the number of segments is set as 8 for Berkeley-MHAD and UTD-MHAD, while 3 for the MMAct. The implementation details for Berkeley-MHAD, UTD-MHAD and MMAct datasets are presented in Table I. All the experiments are conducted with two NVIDIA RTX 2080Ti GPUs using PyTorch [56] framework. For semantic representation extraction of the action class names, we use Glove [50] model and obtain 300 dimensional semantic vectors for each action class. We set hyper-parameters α , β and γ in SAKDN according to the grid-search results.

B. Ablation Study

To evaluate the contribution of the SPAMFM, the GSDM and the SP, we construct three different algorithms based on the SAKDN. **Student (Baseline)**: our student network trained with only RGB videos. **Multi-Teachers**: our teacher networks trained with all wearable-sensor modalities. **SKDN**: our SAKDN without Similarity-Preserving Adaptive Multi-modal Fusion Module (SPAMFM). **SADN**: our SAKDN without Graph-guided Semantically Discriminative Mapping (GSDM) loss. **AKDN**: our SAKDN without semantic preserving for both teacher and student networks. **SAKDN**: our proposed Semantics-aware Adaptive Knowledge Distillation Networks.

The average accuracies on Berkeley-MHAD, UTD-MHAD and MMAct datasets are shown in Table II, III and IV, respectively. In Table II, the SAKDN for six teacher modalities achieve better performance than that of the SKDN, which validates that our proposed SPAMFM can effectively fuse the complementary knowledge among different wearable-sensors. In addition, the SAKDN also performs better than that of the AKDN, this shows that the semantics-preserving part indeed acts as an effective guide for knowledge transfer. The student model with only RGB input (Baseline) achieves better performance than that of the teacher models because the wearable-sensors in Berkeley-MHAD dataset lack color and texture information which may degrade their representative abilities. Introducing different accelerators to the student model improves the performance from 95.32% to 99.33%, which validates the existence of complementary knowledge between wearable-sensors and vision-sensor modalities. In SAKDN, a more significant improvement of performance is achieved than SKDN, SADN and AKDN in video action recognition. In addition, the performance of SKDN, SADN, AKDN are all better than that of the student baseline, which verifies that the SPAMFM, GSDM and SP are complementary and essential.

From Table III, we can see that the teacher-acc, teacher-gyo and multi-teachers using SAKDN outperform the SKDN and AKDN. This validates that the SPAMFM can fully utilize complementary knowledge from multiple teacher modalities and the SP can guide the knowledge transfer using similar semantic relationship between teacher and student modalities. Moreover, the performance of the SKDN, SADN and AKDN are all better than that of the student baseline, which validates the effectiveness of SPAMFM, GSDM and SP. Among SKDN, SADN, AKDN and SAKDN, the SAKDN achieves the best performance and improve the video action recognition performance from 94.87% (baseline) to 98.60%. This validates that our SAKDN can effectively transfer the knowledge from wearable-sensor modalities to vision-sensor modalities by integrating three complementary modules, SPAMFM, GSDM and SP.

To make a fair comparison with other methods in MMAct dataset, we use four different settings [4]. The results for different settings on MMAct dataset is shown in Table IV. In cross-view and cross-scene settings, the multi-teachers achieves better performance than that of the student baseline method. This is because wearable-sensors based action data are more robust to the occlusion and appearance variations

TABLE II: Average accuracies (%) on Berkeley-MHAD dataset. W/O denotes Without, A denotes Accelerator. The number in parenthesis means increased accuracy over the baseline.

Method	Teacher Backbone	Student Backbone	Train Modality	Test Modality	Accuracy
Teacher-Acc1 (SKDN)	VGG16	VGG16	Accelerator 1	Accelerator 1	78.18
Teacher-Acc1 (AKDN)	VGG16	VGG16	Accelerator 1	Accelerator 1	74.90
Teacher-Acc1 (SAKDN)	VGG16	VGG16	Accelerator 1	Accelerator 1	81.09
Teacher-Acc2 (SKDN)	VGG16	VGG16	Accelerator 2	Accelerator 2	75.63
Teacher-Acc2 (AKDN)	VGG16	VGG16	Accelerator 2	Accelerator 2	73.45
Teacher-Acc2 (SAKDN)	VGG16	VGG16	Accelerator 2	Accelerator 2	82.90
Teacher-Acc3 (SKDN)	VGG16	VGG16	Accelerator 3	Accelerator 3	71.63
Teacher-Acc3 (AKDN)	VGG16	VGG16	Accelerator 3	Accelerator 3	68.72
Teacher-Acc3 (SAKDN)	VGG16	VGG16	Accelerator 3	Accelerator 3	75.27
Teacher-Acc4 (SKDN)	VGG16	VGG16	Accelerator 4	Accelerator 4	76.00
Teacher-Acc4 (AKDN)	VGG16	VGG16	Accelerator 4	Accelerator 4	70.54
Teacher-Acc4 (SAKDN)	VGG16	VGG16	Accelerator 4	Accelerator 4	80.36
Teacher-Acc5 (SKDN)	VGG16	VGG16	Accelerator 5	Accelerator 5	52.72
Teacher-Acc5 (AKDN)	VGG16	VGG16	Accelerator 5	Accelerator 5	51.27
Teacher-Acc5 (SAKDN)	VGG16	VGG16	Accelerator 5	Accelerator 5	55.27
Teacher-Acc6 (SKDN)	VGG16	VGG16	Accelerator 6	Accelerator 6	50.90
Teacher-Acc6 (AKDN)	VGG16	VGG16	Accelerator 6	Accelerator 6	46.18
Teacher-Acc6 (SAKDN)	VGG16	VGG16	Accelerator 6	Accelerator 6	54.54
Multi-Teachers (SKDN)	VGG16	VGG16	A1+A2+A3+A4+A5+A6	A1+A2+A3+A4+A5+A6	89.09
Multi-Teachers (AKDN)	VGG16	VGG16	A1+A2+A3+A4+A5+A6	A1+A2+A3+A4+A5+A6	90.54
Multi-Teachers (SAKDN)	VGG16	VGG16	A1+A2+A3+A4+A5+A6	A1+A2+A3+A4+A5+A6	92.00
Student (Baseline)	BNInception	BNInception	RGB videos	RGB videos	95.32
SKDN (W/O SPAMFM)	VGG16	BNInception	A1+A2+A3+A4+A5+A6+RGB	RGB videos	98.11 (+2.79)
SADN (W/O GSDM)	VGG16	BNInception	A1+A2+A3+A4+A5+A6+RGB	RGB videos	98.48 (+3.16)
AKDN (W/O SP)	VGG16	BNInception	A1+A2+A3+A4+A5+A6+RGB	RGB videos	97.63 (+2.31)
SAKDN	VGG16	BNInception	A1+A2+A3+A4+A5+A6+RGB	RGB videos	99.33 (+4.01)

TABLE III: Average accuracies (%) on UTD-MHAD dataset. W/O denotes Without.

Method	Teacher Backbone	Student Backbone	Train Modality	Test Modality	Accuracy
Teacher-Acc (SKDN)	VGG16	VGG16	Accelerator	Accelerator	96.27
Teacher-Acc (AKDN)	VGG16	VGG16	Accelerator	Accelerator	91.84
Teacher-Acc (SAKDN)	VGG16	VGG16	Accelerator	Accelerator	97.66
Teacher-Gyo (SKDN)	VGG16	VGG16	Gyroscope	Gyroscope	93.93
Teacher-Gyo (AKDN)	VGG16	VGG16	Gyroscope	Gyroscope	92.77
Teacher-Gyo (SAKDN)	VGG16	VGG16	Gyroscope	Gyroscope	94.87
Multi-Teachers (SKDN)	VGG16	VGG16	Acc+Gyo	Acc+Gyo	96.27
Multi-Teachers (AKDN)	VGG16	VGG16	Acc+Gyo	Acc+Gyo	97.43
Multi-Teachers (SAKDN)	VGG16	VGG16	Acc+Gyo	Acc+Gyo	98.83
Student (Baseline)	BNInception	BNInception	RGB videos	RGB videos	94.87
SKDN (W/O SPAMFM)	VGG16	BNInception	Acc+Gyo+RGB	RGB videos	97.43 (+2.56)
SADN (W/O GSDM)	VGG16	BNInception	Acc+Gyo+RGB	RGB videos	97.66 (+2.79)
AKDN (W/O SP)	VGG16	BNInception	Acc+Gyo+RGB	RGB videos	96.96 (+2.09)
SAKDN	VGG16	BNInception	Acc+Gyo+RGB	RGB videos	98.60 (+3.73)

TABLE IV: Average accuracies (%) on MMAct dataset. W/O denotes Without.

Method	Teacher Backbone	Student Backbone	Train Modality	Test Modality	Cross Subject	Cross View	Cross Scene	Cross Session
Teacher-Ap (SKDN)	VGG16	VGG16	Acc-phone	Acc-phone	49.54	56.65	55.44	56.81
Teacher-Ap (AKDN)	VGG16	VGG16	Acc-phone	Acc-phone	43.41	52.30	49.22	53.57
Teacher-Ap (SAKDN)	VGG16	VGG16	Acc-phone	Acc-phone	52.34	59.82	57.15	59.38
Teacher-Aw (SKDN)	VGG16	VGG16	Acc-watch	Acc-watch	44.23	49.97	63.26	16.50
Teacher-Aw (AKDN)	VGG16	VGG16	Acc-watch	Acc-watch	37.08	47.08	60.54	16.44
Teacher-Aw (SAKDN)	VGG16	VGG16	Acc-watch	Acc-watch	44.83	53.14	69.42	18.58
Teacher-Gyo (SKDN)	VGG16	VGG16	Gyroscope	Gyroscope	44.70	37.83	50.40	56.14
Teacher-Gyo (AKDN)	VGG16	VGG16	Gyroscope	Gyroscope	41.52	37.74	47.85	51.39
Teacher-Gyo (SAKDN)	VGG16	VGG16	Gyroscope	Gyroscope	52.98	40.86	56.52	59.66
Teacher-Ori (SKDN)	VGG16	VGG16	Orientation	Orientation	42.87	55.09	53.78	57.70
Teacher-Ori (AKDN)	VGG16	VGG16	Orientation	Orientation	40.72	54.20	51.29	53.74
Teacher-Ori (SAKDN)	VGG16	VGG16	Orientation	Orientation	47.12	60.60	58.71	61.56
Multi-Teachers (SKDN)	VGG16	VGG16	Ap+Aw+Gyo+Ori	Ap+Aw+Gyo+Ori	67.45	65.66	78.72	68.77
Multi-Teachers (AKDN)	VGG16	VGG16	Ap+Aw+Gyo+Ori	Ap+Aw+Gyo+Ori	66.64	65.88	79.24	66.53
Multi-Teachers (SAKDN)	VGG16	VGG16	Ap+Aw+Gyo+Ori	Ap+Aw+Gyo+Ori	68.69	68.22	81.61	70.11
Student (Baseline)	BNInception	BNInception	RGB videos	RGB videos	68.41	65.25	56.33	76.79
SKDN (W/O SPAMFM)	VGG16	BNInception	Ap+Aw+Gyo+Ori+RGB	RGB videos	70.38	67.42	57.69	76.96
SADN (W/O GSDM)	VGG16	BNInception	Ap+Aw+Gyo+Ori+RGB	RGB videos	(+1.97)	(+2.17)	(+1.36)	(+0.17)
AKDN (W/O SP)	VGG16	BNInception	Ap+Aw+Gyo+Ori+RGB	RGB videos	69.11	65.16	56.86	79.53
SAKDN	VGG16	BNInception	Ap+Aw+Gyo+Ori+RGB	RGB videos	(+0.70)	(-0.09)	(+0.53)	(+2.74)
AKDN (W/O SP)	VGG16	BNInception	Ap+Aw+Gyo+Ori+RGB	RGB videos	70.63	64.03	62.48	79.63
SAKDN	VGG16	BNInception	Ap+Aw+Gyo+Ori+RGB	RGB videos	(+2.22)	(-1.12)	(+6.15)	(+2.84)
SAKDN	VGG16	BNInception	Ap+Aw+Gyo+Ori+RGB	RGB videos	71.11	68.58	63.41	81.77
SAKDN	VGG16	BNInception	Ap+Aw+Gyo+Ori+RGB	RGB videos	(+2.70)	(+3.33)	(+7.08)	(+4.98)

caused by the camera viewpoint and scene change. Since appearance and texture information are important for action recognition in cross-subject and cross-session settings, the student baseline model fully utilize appearance information and performs better than the multi-teachers which lack tex-

ture and color information to discriminate different human subjects. Base on these observations, we can validate that wearable-sensors and vision-sensors modalities are related and complementary. To be noticed, the performance improvement is negative or limited when using SADN (without GSDM),

TABLE V: Average accuracies (%) on UTD-MHAD dataset for different transfer layers and student backbones, where c denotes convolutional layer, I denotes inception layer.

Student Backbone	Teacher Layers	Student Layers	Acc
BNInception	$\{c_1^2, c_2^2, c_3^3, c_4^3, c_5^3\}$	$\{I5a\}$	97.66
BNInception	$\{c_1^2, c_2^2, c_3^3, c_4^3, c_5^3\}$	$\{I5b\}$	97.90
BNInception	$\{c_1^2, c_2^2, c_3^3, c_4^3, c_5^3\}$	$\{I4d, I5a\}$	97.66
BNInception	$\{c_1^2, c_2^2, c_3^3, c_4^3, c_5^3\}$	$\{I5a, I5b\}$	97.43
BNInception	$\{c_1^2, c_2^2, c_3^3, c_4^3, c_5^3\}$	$\{I4b, I4d, I5a\}$	96.27
BNInception	$\{c_1^2, c_2^2, c_3^3, c_4^3, c_5^3\}$	$\{I4c, I5a, I5b\}$	96.27
BNInception	$\{c_1^2, c_2^2, c_3^3, c_4^3, c_5^3\}$	$\{I3c, I4b, I4d, I5a\}$	98.36
BNInception	$\{c_1^2, c_2^2, c_3^3, c_4^3, c_5^3\}$	$\{I3c, I4c, I5a, I5b\}$	97.90
ResNet18	$\{c_1^2, c_2^2, c_3^3, c_4^3, c_5^3\}$	$\{c_1^1, c_2^1, c_3^1, c_4^1, c_5^1\}$	96.73
ResNet50	$\{c_1^2, c_2^2, c_3^3, c_4^3, c_5^3\}$	$\{c_1^1, c_2^1, c_3^1, c_4^1, c_5^1\}$	98.36
BNInception	$\{c_1^2, c_2^2, c_3^3, c_4^3, c_5^3\}$	$\{I3a, I3c, I4b, I4d, I5a\}$	97.20
ResNet18	$\{c_1^2, c_2^2, c_3^3, c_4^3, c_5^3\}$	$\{c_1^1, c_2^1, c_3^1, c_4^1, c_5^1\}$	95.33
ResNet50	$\{c_1^2, c_2^2, c_3^3, c_4^3, c_5^3\}$	$\{c_1^1, c_2^1, c_3^1, c_4^1, c_5^1, c_8^1, c_9^1\}$	97.90
BNInception	$\{c_1^2, c_2^2, c_3^3, c_4^3, c_5^3\}$	$\{c_2, I3c, I4c, I5a, I5b\}$	98.60

this validates that our proposed GSDM is significantly important for knowledge transfer from wearable-sensors to vision-sensors. In cross-view setting where the appearance of human actions varies a lot because of the changing camera views, the SADN (without GSDM) and the AKDN (without SP) both perform worse than the baseline. While in SAKDN, the performance gain is 3.33%. This shows that the GSDM and the SP are both important for addressing the cross-view challenge. More importantly, our SAKDN outperforms both the multi-teacher models and the baseline model under all settings, which verifies that the SAKDN can effectively exploit complementary knowledge between wearable-sensors and vision-sensors action data and then improve the video action recognition performance in the wild. Among all the settings, the SAKDN performs significantly better than that of the SKDN, SADN and AKDN, which demonstrates that the SPAMFM, GSDM and SP are all complementary and essential.

C. Effect of Different Transfer Layers and Backbones

To validate whether our SAKDN could generalize to different selected layers between teacher and student networks, we evaluate the performance of the SAKDN in UTD-MHAD dataset using different combinations of $\mathcal{L}_{distill}^T$ and $\mathcal{L}_{distill}^S$ in Eq. (21) and (22). In addition, we use different backbones (BNInception, ResNet18 and ResNet50) for student network to measure the generalization ability of SAKDN in different student backbones, as shown in Table V. For BNInception, the performance of using different transfer layers are all better than that of the baseline (94.87%). This validates that our SAKDN can conduct knowledge distillation across different layers between teacher and student networks. To be noticed, for the same backbone, the performance gap of using different numbers of transfer layers is marginal. This shows that our SAKDN can generalize well to different levels of transfer layers. And the performance is the best when we use $\mathcal{L}_{distill}^T = \{c_1^2, c_2^2, c_3^3, c_4^3, c_5^3\}$ and $\mathcal{L}_{distill}^S = \{c_2, I3c, I4c, I5a, I5b\}$. When using different backbones, ResNet18, ResNet50 and BNInception all perform better than the baseline method, which verifies the generalization ability of the SAKDN in different backbones. Among the ResNet18, ResNet50 and BNInception, both

TABLE VI: Parameters sensitivity analysis of α , β , γ on Berkeley-MHAD, UTD-MHAD and MMAAct datasets.

α	β	γ	Berkeley-MHAD	UTD-MHAD	MMAAct (cross-scene)
1	1	1	98.27	95.80	58.32
1	1	0.1	98.39	95.57	60.01
1	0.1	1	98.54	95.80	59.11
1	0.1	0.1	98.72	96.27	56.01
0.1	1	1	97.96	98.60	62.37
0.1	1	0.1	97.90	97.20	62.01
0.1	0.1	1	99.33	96.73	59.47
0.1	0.1	0.1	98.63	97.90	60.79
0.01	1	1	98.39	96.96	59.63
0.01	1	0.1	98.48	96.73	60.92
0.01	0.1	1	98.33	97.66	56.42
0.01	0.1	0.1	98.72	98.13	61.32

the ResNet50 and BNInception achieve better performance than that of the ResNet18, which attributes to the simpler architecture of the ResNet18 for representation learning.

D. Parameter Sensitivity Analysis

There are three hyper-parameters α , β and γ in Eq. (25). To learn how they influence the performance, we conduct the parameter sensitivity analysis on Berkeley-MHAD, UTD-MHAD and MMAAct datasets (cross-scene) using grid-search method. The parameter α get its values in $\{0.01, 0.1, 1\}$, and parameters β and γ get their values in $\{0.1, 1\}$. Table VI shows the performance of our SAKDN by allocating different values to the parameters α , β and γ . We can see that the optimal values for Berkeley-MHAD dataset are $\{0.1, 0.1, 1\}$, while for both UTD-MHAD and MMAAct datasets, the optimal values are $\{0.1, 1, 1\}$. This means that the semantics-preserving should be attached more importance than the soft-target and GSDM, because the semantic relationship contributes a lot among multi-modal feature fusion, knowledge transfer and representation learning for our SAKDN. For parameter α , its optimal values are 0.1 for all datasets. This is because the soft-target loss only conduct knowledge distillation at the last fully-connected layers, while for the GSDM and SP loss, they contribute to the knowledge transfer throughout all layers. For parameter β , the optimal value for Berkeley-MHAD dataset is 0.1, while for both UTD-MHAD and MMAAct datasets, the optimal values are 1. Since the Berkeley-MHAD dataset has six teacher modalities, which is larger than that of the UTD-MHAD and MMAAct datasets. Therefore, β should be set to a moderate value to avoid overfit to any one of the teacher modalities when conducting knowledge distillation.

E. Comparison with State-of-the-Art Methods

We compare the performance of our SAKDN with state-of-the-art knowledge distillation (KD) methods [37]–[40], [57]–[59], vision-based action recognition (VAR) methods [1], [2], [21], and multi-modal action recognition (MMAR) methods [4], [5], [11], [54], [55], [60]–[62]. The comparison results on three datasets are shown in Table VII, Table VIII and Table IX, respectively. For these VAR and KD methods, we use the shared codes, and the parameters are selected based on the default setting. Since [4] is the only existing multi-modal

TABLE VII: Performance comparison on Berkeley-MHAD.

Type	Method	Modality	Accuracy
VAR	TSN [1]	RGB videos	88.19
	TRN [2]	RGB videos	95.32
	TSM [21]	RGB videos	96.87
MMAR	MKL [54]	Accelerators+Depth	97.81
	MPE [60]	Accelerators+Depth	98.10
	MOCAP [61]	Accelerators+Depth	98.38
KD	Logits [57]	Accelerators+RGB Videos	97.93
	Fitnet [58]	Accelerators+RGB Videos	94.38
	ST [37]	Accelerators+RGB Videos	95.99
	AT [38]	Accelerators+RGB Videos	97.99
	RKD [39]	Accelerators+RGB Videos	97.11
	SP [40]	Accelerators+RGB Videos	98.17
	CC [59]	Accelerators+RGB Videos	97.11
Proposed	SAKDN	Accelerators+RGB Videos	99.33

TABLE VIII: Performance comparison on UTD-MHAD.

Type	Method	Modality	Accuracy
VAR	TSN [1]	RGB videos	92.54
	TRN [2]	RGB videos	94.87
	TSM [21]	RGB videos	94.17
MMAR	CRC [55]	Acc+Gyro+Depth	79.10
	CRC-2 [62]	Acc+Gyro+Depth	97.20
	CNN+LSTM [11]	Acc+Gyro+Depth	89.20
	MFLF [5]	Acc+Gyro+RGB Videos	98.20
KD	Logits [57]	Acc+Gyro+RGB Videos	97.20
	Fitnet [58]	Acc+Gyro+RGB Videos	90.20
	ST [37]	Acc+Gyro+RGB Videos	97.90
	AT [38]	Acc+Gyro+RGB Videos	95.80
	RKD [39]	Acc+Gyro+RGB Videos	96.73
	SP [40]	Acc+Gyro+RGB Videos	94.40
	CC [59]	Acc+Gyro+RGB Videos	94.87
Proposed	SAKDN	Acc+Gyro+RGB Videos	98.60

action recognition method for MMAcT dataset which use F-measure to evaluate the performance, we also adopt the F-measure in MMAcT dataset to make a fair comparison.

In Table VII and Table VIII, the SAKDN achieves better performance than all the comparison action recognition methods, multi-modal action recognition methods and knowledge distillation methods. This validates that our SAKDN can effectively improve vision-sensors based action recognition performance by integrating SPAMFM, GSDM and SP into a unified end-to-end adaptive knowledge distillation framework. From Table IX, we can see that the SAKDN performs better than most of the comparison action recognition methods, multi-modal action recognition methods and knowledge distillation methods. To be noticed, the TSM [21] achieves a comparable performance with the SAKDN. This is because the TSM shifts part of the channels along the temporal dimension and thus facilitate information exchanged among neighboring frames. Although the MMAD [4] proposed a multi-modality distillation model to transfer the knowledge from wearable-sensors to vision-sensors, it only use raw one-dimensional time-series sensor signals without considering virtual image generation of wearable-sensor data and the semantic relationship. When using the SAKDN, the performance is the best among all the comparison methods. This validates the effectiveness of our adaptive knowledge distillation framework for sensor-to-vision heterogeneous action recognition by integrating Gramian Angular Field (GAF) based virtual image generation, SPAMFM, GSDM into a unified end-to-end deep learning framework.

V. CONCLUSION

In this paper, we propose an end-to-end knowledge distillation framework, named Semantics-aware Adaptive Knowledge

TABLE IX: Performance comparison on MMAcT.

Method	Modality	Cross subject	Cross view	Cross scene	Cross session
TSN [1]	RGB videos	59.50	54.37	51.21	68.65
TRN [2]	RGB videos	66.56	65.51	60.03	71.95
TSM [21]	RGB videos	70.12	67.22	66.04	81.32
SMD [37]	A+RGB	63.89	66.31	61.56	71.23
MMD [4]	A+G+O+RGB	64.33	68.19	62.23	72.08
MMAD [4]	A+G+O+RGB	66.45	70.33	64.12	74.58
Logits [57]	A+G+O+RGB	65.06	60.94	57.92	74.14
Fitnet [58]	A+G+O+RGB	33.96	30.14	18.88	35.87
ST [37]	A+G+O+RGB	64.45	60.39	58.72	74.80
AT [38]	A+G+O+RGB	65.59	60.30	55.92	74.28
RKD [39]	A+G+O+RGB	65.54	61.67	55.38	75.05
SP [40]	A+G+O+RGB	65.16	60.76	57.48	74.41
CC [59]	A+G+O+RGB	65.60	59.59	59.65	73.98
SAKDN	A+G+O+RGB	77.23	73.48	66.38	82.77

Distillation Networks (SAKDN), to adaptively distill the complementary knowledge from multiple wearable-sensors (teachers) to the vision-sensor (student), and concurrently improve the action recognition performance in vision-sensor modality (videos). To fully utilize the complementary knowledge from multiple teachers, we propose a novel plug-and-play module, named Similarity-Preserving Adaptive Multi-modal Fusion Module (SPAMFM), which integrates intra-modality similarity, semantic embeddings and multiple relational knowledge to learn the global context representation and recalibrate the channel-wise features adaptively in each teacher network. To effectively exploit and transfer the knowledge of multiple well-trained teachers to the student, we propose a novel knowledge distillation loss, named Graph-guided Semantically Discriminative Mapping (GSDM) loss, which utilizes graph-guided ablation analysis to produce a visual explanation highlighting the important regions for predicting the semantic concept, and concurrently preserving respective interrelations of data for each modality. Extensive experiments on three benchmarks demonstrate the effectiveness of our SAKDN for adaptive knowledge transfer from wearable-sensors to vision-sensors.

REFERENCES

- [1] L. Wang, Y. Xiong, Z. Wang, Y. Qiao, D. Lin, X. Tang, and L. Van Gool, "Temporal segment networks for action recognition in videos," *IEEE transactions on pattern analysis and machine intelligence*, vol. 41, no. 11, pp. 2740–2755, 2018.
- [2] B. Zhou, A. Andonian, A. Oliva, and A. Torralba, "Temporal relational reasoning in videos," in *Proceedings of the European Conference on Computer Vision*, 2018, pp. 803–818.
- [3] X. Wang, R. Girshick, A. Gupta, and K. He, "Non-local neural networks," in *Proceedings of the IEEE conference on computer vision and pattern recognition*, 2018, pp. 7794–7803.
- [4] Q. Kong, Z. Wu, Z. Deng, M. Klinkigt, B. Tong, and T. Murakami, "MmacT: A large-scale dataset for cross modal human action understanding," in *Proceedings of the IEEE International Conference on Computer Vision*, 2019, pp. 8658–8667.
- [5] M. Ehatisham-Ul-Haq, A. Javed, M. A. Azam, H. M. Malik, A. Irtaza, I. H. Lee, and M. T. Mahmood, "Robust human activity recognition using multimodal feature-level fusion," *IEEE Access*, vol. 7, pp. 60736–60751, 2019.
- [6] W. Jiang and Z. Yin, "Human activity recognition using wearable sensors by deep convolutional neural networks," in *Proceedings of the 23rd ACM international conference on Multimedia*, 2015, pp. 1307–1310.
- [7] J. Wannenburg and R. Malekian, "Physical activity recognition from smartphone accelerometer data for user context awareness sensing," *IEEE Transactions on Systems, Man, and Cybernetics: Systems*, vol. 47, no. 12, pp. 3142–3149, 2016.
- [8] J. Wang, Y. Chen, S. Hao, X. Peng, and L. Hu, "Deep learning for sensor-based activity recognition: A survey," *Pattern Recognition Letters*, vol. 119, pp. 3–11, 2019.

- [9] K. Wang, J. He, and L. Zhang, "Attention-based convolutional neural network for weakly labeled human activities recognition with wearable sensors," *IEEE Sensors Journal*, vol. 19, no. 17, pp. 7598–7604, 2019.
- [10] Z. Ahmad and N. Khan, "Human action recognition using deep multilevel multimodal (m2) fusion of depth and inertial sensors," *IEEE Sensors Journal*, 2019.
- [11] N. Dawar, S. Ostadabbas, and N. Kehtarnavaz, "Data augmentation in deep learning-based fusion of depth and inertial sensing for action recognition," *IEEE Sensors Letters*, vol. 3, no. 1, pp. 1–4, 2018.
- [12] H. Wei, R. Jafari, and N. Kehtarnavaz, "Fusion of video and inertial sensing for deep learning-based human action recognition," *Sensors*, vol. 19, no. 17, p. 3680, 2019.
- [13] N. C. Garcia, P. Morerio, and V. Murino, "Learning with privileged information via adversarial discriminative modality distillation," *IEEE transactions on pattern analysis and machine intelligence*, 2019.
- [14] Z. Wang and T. Oates, "Imaging time-series to improve classification and imputation," in *Twenty-Fourth International Joint Conference on Artificial Intelligence*, 2015.
- [15] J. K. Aggarwal and M. S. Ryou, "Human activity analysis: A review," *ACM Computing Surveys (CSUR)*, vol. 43, no. 3, pp. 1–43, 2011.
- [16] H. Wang and C. Schmid, "Action recognition with improved trajectories," in *Proceedings of the IEEE international conference on computer vision*, 2013, pp. 3551–3558.
- [17] S. Ji, W. Xu, M. Yang, and K. Yu, "3d convolutional neural networks for human action recognition," *IEEE transactions on pattern analysis and machine intelligence*, vol. 35, no. 1, pp. 221–231, 2012.
- [18] K. Simonyan and A. Zisserman, "Two-stream convolutional networks for action recognition in videos," in *Advances in neural information processing systems*, 2014, pp. 568–576.
- [19] D. Tran, L. Bourdev, R. Fergus, L. Torresani, and M. Paluri, "Learning spatiotemporal features with 3d convolutional networks," in *Proceedings of the IEEE international conference on computer vision*, 2015, pp. 4489–4497.
- [20] L. Wang, Y. Xiong, Z. Wang, Y. Qiao, D. Lin, X. Tang, and L. Van Gool, "Temporal segment networks: Towards good practices for deep action recognition," in *European conference on computer vision*, 2016, pp. 20–36.
- [21] J. Lin, C. Gan, and S. Han, "Tsm: Temporal shift module for efficient video understanding," in *Proceedings of the IEEE International Conference on Computer Vision*, 2019, pp. 7083–7093.
- [22] J. Liu, A. Shahroudy, M. L. Perez, G. Wang, L.-Y. Duan, and A. K. Chichung, "Ntu rgb+d 120: A large-scale benchmark for 3d human activity understanding," *IEEE transactions on pattern analysis and machine intelligence*, 2019.
- [23] W. Li, L. Chen, D. Xu, and L. Van Gool, "Visual recognition in rgb images and videos by learning from rgb-d data," *IEEE transactions on pattern analysis and machine intelligence*, vol. 40, no. 8, pp. 2030–2036, 2017.
- [24] S. Yan, Y. Xiong, and D. Lin, "Spatial temporal graph convolutional networks for skeleton-based action recognition," in *Thirty-second AAAI conference on artificial intelligence*, 2018.
- [25] F. Meng, H. Liu, Y. Liang, J. Tu, and M. Liu, "Sample fusion network: an end-to-end data augmentation network for skeleton-based human action recognition," *IEEE Transactions on Image Processing*, vol. 28, no. 11, pp. 5281–5295, 2019.
- [26] Y. Liu, Z. Lu, J. Li, T. Yang, and C. Yao, "Global temporal representation based cnns for infrared action recognition," *IEEE Signal Processing Letters*, vol. 25, no. 6, pp. 848–852, 2018.
- [27] O. D. Lara and M. A. Labrador, "A survey on human activity recognition using wearable sensors," *IEEE communications surveys & tutorials*, vol. 15, no. 3, pp. 1192–1209, 2012.
- [28] F. Setiawan, B. N. Yahya, and S.-L. Lee, "Deep activity recognition on imaging sensor data," *Electronics Letters*, vol. 55, no. 17, pp. 928–931, 2019.
- [29] Y. Liu, Z. Lu, J. Li, and T. Yang, "Hierarchically learned view-invariant representations for cross-view action recognition," *IEEE Transactions on Circuits and Systems for Video Technology*, vol. 29, no. 8, pp. 2416–2430, 2018.
- [30] L. Wang, Z. Ding, Z. Tao, Y. Liu, and Y. Fu, "Generative multi-view human action recognition," in *Proceedings of the IEEE International Conference on Computer Vision*, 2019, pp. 6212–6221.
- [31] A. Shahroudy, T.-T. Ng, Y. Gong, and G. Wang, "Deep multimodal feature analysis for action recognition in rgb+d videos," *IEEE transactions on pattern analysis and machine intelligence*, vol. 40, no. 5, pp. 1045–1058, 2017.
- [32] Y. Liu, Z. Lu, J. Li, C. Yao, and Y. Deng, "Transferable feature representation for visible-to-infrared cross-dataset human action recognition," *Complexity*, vol. 2018, 2018.
- [33] F. Yu, X. Wu, J. Chen, and L. Duan, "Exploiting images for video recognition: Heterogeneous feature augmentation via symmetric adversarial learning," *IEEE Transactions on Image Processing*, vol. 28, no. 11, pp. 5308–5321, 2019.
- [34] Y. Liu, Z. Lu, J. Li, T. Yang, and C. Yao, "Deep image-to-video adaptation and fusion networks for action recognition," *IEEE Transactions on Image Processing*, vol. 29, pp. 3168–3182, 2020.
- [35] C. Chen, R. Jafari, and N. Kehtarnavaz, "Improving human action recognition using fusion of depth camera and inertial sensors," *IEEE Transactions on Human-Machine Systems*, vol. 45, no. 1, pp. 51–61, 2014.
- [36] H. R. V. Joze, A. Shaban, M. L. Iuzzolino, and K. Koishida, "Mmtm: Multimodal transfer module for cnn fusion," in *Proceedings of the IEEE Conference on Computer Vision and Pattern Recognition*, 2020, pp. 13 289–13 299.
- [37] G. Hinton, O. Vinyals, and J. Dean, "Distilling the knowledge in a neural network," *arXiv preprint arXiv:1503.02531*, 2015.
- [38] S. Zagoruyko and N. Komodakis, "Paying more attention to attention: Improving the performance of convolutional neural networks via attention transfer," in *International Conference on Learning Representations*, 2017.
- [39] W. Park, D. Kim, Y. Lu, and M. Cho, "Relational knowledge distillation," in *Proceedings of the IEEE Conference on Computer Vision and Pattern Recognition*, 2019, pp. 3967–3976.
- [40] F. Tung and G. Mori, "Similarity-preserving knowledge distillation," in *Proceedings of the IEEE International Conference on Computer Vision*, 2019, pp. 1365–1374.
- [41] J. Hoffman, S. Gupta, and T. Darrell, "Learning with side information through modality hallucination," in *Proceedings of the IEEE Conference on Computer Vision and Pattern Recognition*, 2016, pp. 826–834.
- [42] N. C. Garcia, P. Morerio, and V. Murino, "Modality distillation with multiple stream networks for action recognition," in *Proceedings of the European Conference on Computer Vision (ECCV)*, 2018, pp. 103–118.
- [43] N. Crasto, P. Weinzaepfel, K. Alahari, and C. Schmid, "Mars: Motion-augmented rgb stream for action recognition," in *Proceedings of the IEEE Conference on Computer Vision and Pattern Recognition*, 2019, pp. 7882–7891.
- [44] K. Simonyan and A. Zisserman, "Very deep convolutional networks for large-scale image recognition," in *International Conference on Learning Representations*, 2015.
- [45] H. Zhao, J. Jia, and V. Koltun, "Exploring self-attention for image recognition," in *Proceedings of the IEEE Conference on Computer Vision and Pattern Recognition*, 2020, pp. 10 076–10 085.
- [46] J. Hu, L. Shen, and G. Sun, "Squeeze-and-excitation networks," in *Proceedings of the IEEE conference on computer vision and pattern recognition*, 2018, pp. 7132–7141.
- [47] A. S. Morcos, D. G. T. Barrett, N. C. Rabinowitz, and M. Botvinick, "On the importance of single directions for generalization," in *International Conference on Learning Representations*, 2018.
- [48] B. Zhou, Y. Sun, D. Bau, and A. Torralba, "Revisiting the importance of individual units in cnns via ablation," *CoRR*, vol. abs/1806.02891, 2018.
- [49] S. Desai and H. G. Ramaswamy, "Ablation-cam: Visual explanations for deep convolutional network via gradient-free localization," in *IEEE Winter Conference on Applications of Computer Vision*, 2020, pp. 972–980.
- [50] J. Pennington, R. Socher, and C. D. Manning, "Glove: Global vectors for word representation," in *Proceedings of the conference on empirical methods in natural language processing*, 2014, pp. 1532–1543.
- [51] F. R. Chung and F. C. Graham, *Spectral graph theory*. American Mathematical Soc., 1997, no. 92.
- [52] Y. Liu, J. Lee, M. Park, S. Kim, E. Yang, S. J. Hwang, and Y. Yang, "Learning to propagate labels: Transductive propagation network for few-shot learning," in *International Conference on Learning Representations*, 2019.
- [53] R. R. Selvaraju, M. Cogswell, A. Das, R. Vedantam, D. Parikh, and D. Batra, "Grad-cam: Visual explanations from deep networks via gradient-based localization," in *Proceedings of the IEEE international conference on computer vision*, 2017, pp. 618–626.
- [54] F. Ofli, R. Chaudhry, G. Kurillo, R. Vidal, and R. Bajcsy, "Berkeley mhad: A comprehensive multimodal human action database," in *IEEE Workshop on Applications of Computer Vision*, 2013, pp. 53–60.

- [55] C. Chen, R. Jafari, and N. Kehtarnavaz, "Utd-mhad: A multimodal dataset for human action recognition utilizing a depth camera and a wearable inertial sensor," in *IEEE International conference on image processing*, 2015, pp. 168–172.
- [56] A. Paszke, S. Gross, F. Massa, A. Lerer, J. Bradbury, G. Chanan, T. Killeen, Z. Lin, N. Gimeshin, L. Antiga *et al.*, "Pytorch: An imperative style, high-performance deep learning library," in *Advances in Neural Information Processing Systems*, 2019, pp. 8024–8035.
- [57] J. Ba and R. Caruana, "Do deep nets really need to be deep?" in *Advances in neural information processing systems*, 2014, pp. 2654–2662.
- [58] A. Romero, N. Ballas, S. E. Kahou, A. Chassang, C. Gatta, and Y. Bengio, "Fitnets: Hints for thin deep nets," in *International Conference on Learning Representations*, 2015.
- [59] B. Peng, X. Jin, J. Liu, D. Li, Y. Wu, Y. Liu, S. Zhou, and Z. Zhang, "Correlation congruence for knowledge distillation," in *Proceedings of the IEEE International Conference on Computer Vision*, 2019, pp. 5007–5016.
- [60] A. Shafaei and J. J. Little, "Real-time human motion capture with multiple depth cameras," in *2016 13th Conference on Computer and Robot Vision (CRV)*. IEEE, 2016, pp. 24–31.
- [61] E. P. Ijjina and C. K. Mohan, "Human action recognition based on mocap information using convolution neural networks," in *2014 13th International Conference on Machine Learning and Applications*. IEEE, 2014, pp. 159–164.
- [62] C. Chen, R. Jafari, and N. Kehtarnavaz, "A real-time human action recognition system using depth and inertial sensor fusion," *IEEE Sensors Journal*, vol. 16, no. 3, pp. 773–781, 2015.